Aerosol and Air Quality Research, 18: 1746–1755, 2018

ISSN: 1680-8584 print / 2071-1409 online
doi: 10.4209/aaqr.2018.02.0047

Thermophoresis and Brownian Motion Effects on Nanoparticle Deposition Inside a 90° Square Bend Tube

Zhao-Qin Yin, Xian-Feng Li, Fu-Bing Bao*, Cheng-Xu Tu, Xiao-Yan Gao

Institute of Fluid Mechanics, China Jiliang University, Hangzhou 310018, China

ABSTRACT

Aerosol nanoparticle deposition onto a surface under a temperature gradient is commonly applied in the chemical and medical industries. In this study, a numerical investigation with a two-phase model is used to investigate the deposition characteristics of nanosized particles in a 90° square bend. The effects of variations in the gas phase physical parameters, such as density, viscosity, and thermal diffusivity with changing temperatures are studied. The main forces acting on the particles are the drag forces, Brownian forces, and thermophoretic forces. A discrete phase model (DPM) based on the FLUENT software is used to investigate particle transfer. The results show that in a temperature gradient flow, particles move towards the colder wall, and some of them strike and deposit onto its surface. The particle deposition efficiency increases with the temperature gradient rising. The Brownian force plays a more important role in particle deposition when smaller particles are used. Because of inertia and gravity, particle deposition on the four surfaces of a 90° square bend tube is inhomogeneous. The deposition efficiency on the floor surface increases with increasing particle diameter. On the contrary, larger particles decrease the deposition efficiency on the ceiling surface.

***Keywords*:** Aerosol nanoparticle; Thermophoretic force; Brownian force; Deposition.

NOMENCLATURE

C	air thermal conductivity (W m^{-1} K^{-1})
Cp	particle thermal conductivity (W m^{-1} K^{-1})
Cc	the slip correction factor
D	the side length of inlet (m)
D_B	Brownian diffusion coefficient (m^2 s^{-1})
De	Dean number
D_T	thermophoretic diffusion coefficient (m^2 s^{-1})
d_p	diameter of the nanoparticle (m)
f	unit mass force (N kg^{-1})
F_B	the Brownian force (N)
F_D	the drag force (N)
F_T	the thermophoretic force (N)
g	Gravitational acceleration (m s^{-2})
K	the Boltzmann constant (= 1.381 × 10^{-23} J K^{-1})
Kn	Knudsen number
m	the mass (kg)
n	the deposition efficiency
N	the number of particle
N_{BT}	the ratio of Brownian diffusivity to thermophoretic diffusivity
p	pressure (Pa)
R_0	the curvature ratio of the elbow (m)
R_1	the internal diameter of the elbow (m)
R_2	the external diameter of the elbow (m)
Re	Reynolds number
T	the time (S)
T	temperature (K)
u	velocity (m s^{-1})
x, y, z	dimensional Cartesian coordinates (m)

Greek letters

α	thermal diffusivity (m^2 s)
∇	Gradient
μ	dynamic viscosity (kg m^{-1} s^{-1})
ν	kinematic viscosity (m^2 s^{-1})
ξ_0	Gaussian random numbers
ρ	density (kg m^{-3})

Subscripts

B	Brownian
f	fluid
p	particle
T	thermophoresis

INTRODUCTION

Aerosol nanoparticle deposition in bend surfaces is adopted in diverse scenarios, such as chemical and medical industries, environmental engineering, instrument and

* Corresponding author.
E-mail address: dingobao@cjlu.edu.cn

semiconductor engineering (Garoosi *et al*., 2015a; Gupta *et al*., 2016; Tiwari *et al*., 2017; Zhu *et al*., 2017; Chen *et al*., 2018). In transport processes, it is important to understand the physics and the process of particle motion, which is directly related to particle deposition on the container walls and can result in scale formation, fouling, and reduction of heat transfer performance (Stapleton *et al*., 2000; Mädler and Friedlander, 2007; Murgia *et al*., 2016; Schubert *et al*., 2017).

The physical mechanisms governing the movement and deposition of aerosol particles are complex. Numerous factors contribute to particle deposition on the surface of a tube, such as gravitation, electrostatic interactions, inertial impaction, turbulence, and Brownian diffusion (Zhang and Friedlander, 2000; Ketzel and Berkowicz, 2004). Of these, Brownian particle diffusion is more significant for nanosized particles than for larger particles, leading to higher deposition rates for nanoparticles (Li *et al*., 2010). When there is a gradient in fluid temperature, particles tend to move from the higher-temperature region to the lower-temperature region via thermophoresis (Rahman *et al*., 2012). Shimada *et al.* (1993) first determined the deposition velocities for monodisperse aerosol particles with diameters of 10–40 nm at two cross-sections of pipe by considering Brownian and turbulent diffusive deposition. Apart from this, he (1994) also found that thermophoretic deposition was enhanced by the increase in the wall temperature variation, but this phenomenon did not depend on the particle. Shams (2000) and Ahmadi (2001) studied the effects of turbulent, gravitational, Brownian, and lift forces, and determined the deposition velocity and particle deposition rate. Tsai *et al*. (2004) assessed various particle deposition effects so that thermophoretic deposition alone was measured accurately. Buongiorno (2006) investigated different slip mechanisms between nanoparticles and base fluids. He concluded that Brownian diffusion and thermophoresis are the only important slip mechanisms in laminar flow. Zahmatkesh (2008) showed that depending upon temperature gradient, varying degrees of thermophoretic and Brownian diffusion may contribute to particle deposition. Lin *et al.* (2009a, b) studied the transport and deposition of nanoparticles in bends for different angular velocities, Dean numbers, and Schmidt numbers. Healy and Young (2010) critically discussed the various expressions for the thermophoretic force on an aerosol particle. Chiou *et al*. (2011) considered the particle transport mechanisms of Brownian and turbulent diffusion, eddy impaction, particle inertia, and thermophoresis, and discovered that in the presence of a temperature gradient near the container wall, the thermophoretic effect plays a more active role in movement through the viscous sublayer compared to the other mechanisms, and the smallest particles benefit most from this effect because of their low inertia. Abarham *et al*. (2013) developed an axisymmetric model to predict thermophoretic deposition, and found that the axisymmetric model estimated the deposited mass more accurately. Guha and Samanta (2014) examined various thermophoresis expressions and computed the deposition of nano- to micro-sized particles on both vertical and horizontal surfaces. Lin *et al*. (2010, 2014) studied aerosol particle deposition under the combined effects of Brownian diffusion, turbulent diffusion, particle coagulation, and breakage with a moment method.

In the above mentioned references there are two basically different approaches to study the moving of particles suspension in fluid, Eulerian – Eulerian and Eulerian - Lagrangian approaches. The Eulerian approach deals with the concentration of particles and states the overall diffusion and convection of a number of particles whereas Lagrangian approach deals with the individual particle and calculates the trajectory of each particle separately (Saidi *et al.*, 2014; Garoosi *et al.*, 2016). Therefore, the calculations with Lagrangian approach are quite more time consuming than Eulerian approach. But the studies of Vegendla (2011) show that slip velocity between the fluid and particles may exist due to several factors such as Brownian, thermophoresis, gravity forces etc., so Lagrangian models agreed well with experimental data; therefore it seems that the Eulerian - Lagrangian approach is better model to apply the nanoparticle.

Despite the attention paid to aerosol particle deposition under the effects of either Brownian diffusion or thermophoresis, there is a lack of study on nanoparticle motion and deposition in a bend under the combined effects of these forces. The competition between Brownian diffusion and thermophoresis affects the particle distribution in the cross-section of the pipe, and thus, changing the deposition efficiency is not explicit. The most severe abrasion and corrosion in a tube always occurs at a bend. The internal flow characteristics in a bend are different and more complex than those in the straight pipe, which changes the deposition rates and locations of the particles. The deposition of micro-sized aerosol particles in a 90° bend has been studied extensively, but there are fewer studies about nanosized particles with temperature gradients in bends. For a better understanding of the mechanism of nanoparticle flow in a temperature gradient at a bend, a numerical investigation with a two-phase model is presented here to model the deposition characteristics of nanosized particles in a 90° square bend tube. The main goal of this work is to explore the different effects of Brownian and thermophoretic motions on the process of nanoparticle motion.

MATHEMATICAL MODEL

Governing Equations of the Gas Phase

In this study, the continuous phase of gas is calculated using Euler approach along with a finite-volume method. It is assumed that the gas is incompressible, Newtonian, and continuous. The fluid flow field in a pipe is calculated by solving the governing partial differential equations of mass, momentum, and energy, which are:

$$\nabla \cdot \mathbf{u} = 0 \tag{1}$$

$$\frac{\partial \mathbf{u}}{\partial t} + \mathbf{u} \cdot \nabla \mathbf{u} = -\nabla p + \rho \nu \nabla^2 \mathbf{u} \tag{2}$$

$$\frac{\partial T}{\partial t} + \mathbf{u} \cdot \nabla T = \alpha \nabla^2 T \tag{3}$$

where **u** is the fluid velocity vector, p the gas pressure, T the temperature, t the time respectively. v is the viscosity of gas, ρ the density of the fluid, α the thermal diffusivity, and all of them change with the gas temperature. The effects of temperature on density, viscosity and thermal diffusivity in the range 0–100°C can be described using the polynomial functions of experimental data as (Incropera and DeWitt, 2002):

$$\rho = 4.361 - 0.021T + 5.005 \times 10^{-5}T^2 - 5.818 \times 10^{-8}T^3 + 2.654 \times 10^{-11}T^4 \tag{4}$$

$$\mu = (-2.604 + 0.04T - 2 \times 10^{-4}T^2 + 3 \times 10^{-7}T^3 - 2 \times 10^{-10}T^4) \times 10^{-5} \tag{5}$$

$$a = 0.62 - 7.9 \times 10^{-3}T + 3.9 \times 10^{-5}T^2 - 8 \times 10^{-8}T^3 + 6 \times 10^{-11}T^4 \tag{6}$$

Equation of Particle Motion

The particle migration is affected by many slip mechanisms, such as fluid drag, inertia, Brownian motion, gravity, thermophoresis, and so on. According to Buongiorno's (2006) study, nanoparticles can be in motion with transport fluid, while maintaining a slip velocity relative to the fluid. For nanoparticles, the Brownian force and thermophoretic force are the important slip mechanisms in the transfer process.

In this study, the particle motion is simulated by a Lagrangian method. Considering both precision and efficiency, the particle phase is taken into account the following three assumptions. Firstly, it is assumed that particles are smooth, spherical, dilute and minute. Secondary, for numerous small particles, a direct simulation of inter-particle collisions is not practicable due to the high computational cost and the large storage requirements, and consequently the inter-particle effects may be ignored. It is reasonable considering the particle concentration and size due to Sommerfeld' study (2001). Thirdly, the walls are considered to be perfectly absorbing, so that when a particle strikes a wall, it adheres to the surface. Therefore, the particle influence on the fluid can be neglected.

Fig. 1 shows the forces acting on a particle in a fluid flow with a temperature gradient. The flow drag force, Brownian force, and thermophoretic force are affecting a particle. The small black dots represent the gas molecules, which are randomly fluctuating. The velocity is a function of the gas temperature. The thermophoretic force is proportional to the temperature gradient, so that the wider the temperature gradient, the larger the thermophoretic force. The thermophoretic force causes nanoparticle migration across the fluid in the opposite direction of the temperature gradient. The fluid drag force is proportional to the air velocity and carries the particle through the pipe (Garoosi *et al*., 2015b).

Based on the forces effect on the particle and Newton's second law, the dynamics equation of motion for the particles in a gas-particle two phases flow is given by (Garoosi and Talebi, 2017):

$$m_p \frac{du_p}{dt} = gV_p\left(\rho - \rho_p\right) + F_D + F_B + F_T \tag{7}$$

where m_p is the mass of the particle, ρ_p is the density of the particles. u_p is the particle velocity, F_D the drag force, F_B the Brownian force, and F_T the thermophoretic force respectively.

The expression for the drag force is:

$$F_D = 3\pi\mu u d_p / C_c \tag{8}$$

where μ is the fluid dynamic viscosity. d_p is the diameter of the nanoparticle, and Cc the Cunningham correction factor,

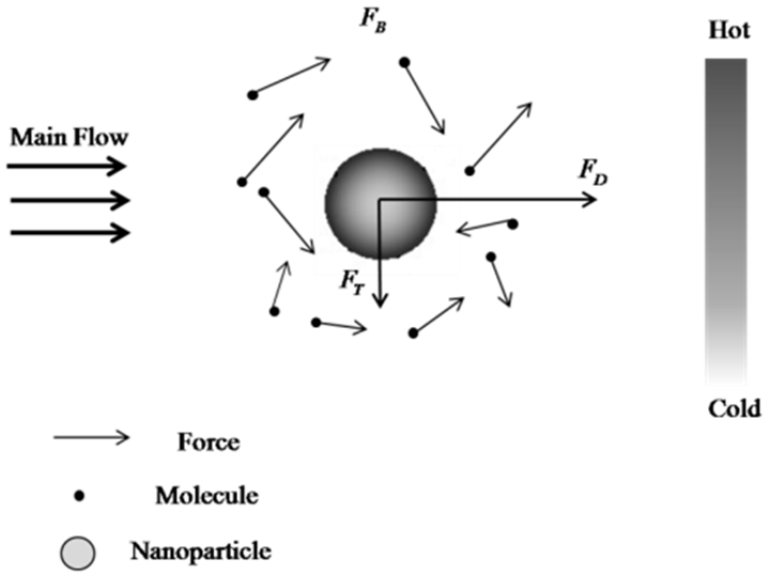

Fig. 1. Schematic of forces effecting.

which can be expressed as a function of Knudsen number (Kn). Kn represents the mass, momentum and heat transfer between a particle and its surrounding gas molecules. The expression of Kn is the ratio of gas molecule mean free path to half nanoparticle diameter. When the particle size is in the region of $0.06 < Kn < 10$, the slip correction factor Cc has the following expression:

$$Cc = 1 + Kn[1.257 + 0.4\exp(-1.1/Kn)] \quad (9)$$

The amplitude of a random Brownian force F_B was expressed as a Gaussian white noise process following Kim and Zydney (2004), using the expression:

$$F_B = \xi_0 \sqrt{\frac{12\pi\mu d_p KT}{\Delta t}} \quad (10)$$

where K (= 1.381×10^{-23} J K^{-1}) is the Boltzmann constant, Δt is the time elapsed, and ξ_0 is a zero-mean variant from a Gaussian probability density function. The independent values of ξ_0 in x, y, and z components at each time evaluate the random instantaneous Brownian force of three directions.

For particles in the transition and continuum regions, the dynamics equation in a temperature gradient flow field is rather difficult to be described theoretically. The thermophoretic force was firstly formulated by Brock (1962) using a fluid mechanics method with slip-corrected boundary conditions, and then improved by Talbot *et al*. (1980). In this numerical simulation the thermophoretic force is expressed as:

$$F_T = 4.5\pi \frac{\mu^2}{\rho} d_p \frac{1}{1+3Kn} \frac{\frac{C}{C_p} + 2.48Kn}{1 + 2\frac{C}{C_p} + 4.48\frac{C}{C_p}} \frac{\nabla T}{T} \quad (11)$$

where C and C_p are the thermal conductivity of air and the particle, respectively.

Physical Model and Boundary Conditions

The geometrical model of a 90° square cross-section bend studied in this paper is shown in Fig. 2. The square tube consists of a horizontal inlet section, a bending section, and a vertical downward outlet section, while the side length of cross section is 10 mm. To enable a fully developed flow state, a horizontal inlet section and a vertical straight outlet section are mounted to the 90° bend, and both lengths are 20 D. The curvature ratio $R_0 = (R_1 + R_2)/2\ D = 10$, R_1, R_2, and D are shown in Fig. 2.

The velocity inlet boundary condition was defined to be the bend inlet. The temperature and velocity of gas and

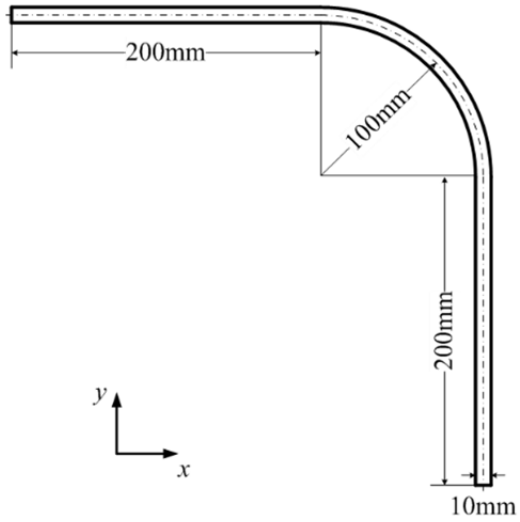

Fig. 2. Sketch of the simulation geometry.

number and diameter of the particle were specified at the inlet boundary. The bend outlet boundary condition was outflow, and a no-slip boundary condition was used for the pipe surfaces. The wall temperature was at constant 293 K. The thermo-physical properties of the air and solid particles at $T = 293$ K as listed in Table 1.

Numerical Grid Refinement and Verification

The flow, including velocity and temperature distribution, through a bend has been simulated using a commercial CFD package FLUENT platform with UDF function. The governing partial differential equations were converted into algebraic equations by the finite volume method (FVM). The second-order central difference scheme is used for the diffusion terms while the convective terms are formulated by the QUICK scheme of Spalding. The semi-implicit method for pressure-linked equations (SIMPLE) is adopted to couple the pressure and velocity fields (Garoosi *et al*., 2013, 2017). The convergence criteria reduced the maximum relative error in the values of all dependent variables between two successive iterations below 10^{-6}.

The entire computational region was structured by the hexahedral mesh. To obtain an optimal grid distribution with minimal computational time, grid independence study is performed at T = 293 K and d_p = 80 nm with inlet velocity $u = 0.6$ m s^{-1}. The result has been shown in Table 2. The deviations between the results for particle deposition efficiency (n) inside the tube obtained for grid number 959,616 and 1455,737 was less than 1% as depicted in Table 2. As a result, throughout this study, the number of discrete grids was 959,616. All the particle parcels are tracked by the Lagrangian approach with discrete phase model (DPM). For DPM all particles of every computational

Table 1. Thermo-physical properties of the air and solid particles at $T = 293$ K.

	ρ (kg m^{-3})	C (w mK^{-1})	α (m^2 s)	μ (kg m^{-1} s^{-1})
air	1.205	0.0259	2.14×10^{-5}	18.1×10^{-6}
particle	1225	1.51	/	/

Table 2. Effect of the grid size on the particle deposition efficiency n at T = 293 K and d_p = 80 nm.

Grid number	364461	603911	9599616	1455737
n	0.129	0.120	0.114	0.113

cell are separated into a number of parcels. One simulation particle in each parcel represents all real particles in that group. There are 1764 grids in the square tube section surface, which means that the computational parcel number is 1764. However, the realistic number of nanoparticles is acquired according to the number of parcels and the mass flow. With the changing of the particle volume concentration, the mass flow has been changed accordingly. For the volume concentration of particles in the flow is smaller than 0.01%, one-way coupling can be assumed on the basis of the prior three assumptions. Therefore, each motion of particles is affected by the gas flow, but the gas flow is not affected by the presence of the nanoparticles.

Fig. 3 shows the theoretical and numerical velocity distributions of fluid flow in the tube before the elbow under adiabatic condition. The results from Fig. 3 are in good agreement with the given Poiseuille theoretical velocity distribution, indicating the validity of the flow simulation.

RESULTS AND DISCUSSION

Continuous Flow Field

The dispersion and deposition of particles in fluid flow were affected by a variety of different factors, including the flow Reynolds number, particle diameter, and initial conditions. Particle behavior in a continuous bend flow field depends on the flow Reynolds number and the curvature ratio, which can be combined into another parameter, Dean number (De). De replaces the Reynolds number for flow in a curved pipe (Yook and Pui, 2006). The Dean number is calculated using De = Re × $(1/R_0)^{0.5}$. In this paper the Dean number, which changed with the inlet temperature and velocity, is smaller than 200. The fluid field is in laminar flow state.

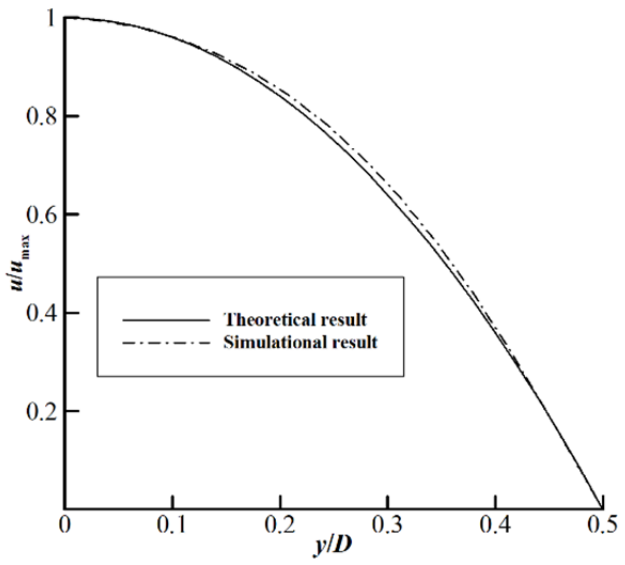

Fig. 3. The velocity distribution at x = 20 D.

Fig. 4 displays the streamlines at a 45° deflection in a cross-section of the bend at De = 129.9. The streamlines in the plane provide an indication that there is a secondary flow in the bend, and they show that the flow field is fully parallel to the plane. The pair of counter rotation helical vortices are formed because of the centrifugally caused by pressure gradient driving the faster moving fluid in the core outward, while driving the slower moving fluid near the wall inward. Thus, the flow is dominated by centrifugal force. The secondary flow in the bend has been previously reported (Breuer *et al*., 2006).

Fig. 5 shows the velocity distribution with different temperatures at the same pipe inlet velocity. The results indicate the flow velocity is fully parallel to the plane. With increasing gas temperature, the density and viscosity of gas are changed, and the velocity distribution changes accordingly. The velocity gradient decreases with the increasing of the inlet air temperature. Temperature and temperature gradient are the main factors influencing the Brownian and thermophoretic forces, which in turn affect the particle movement. Fig. 6 shows the temperature gradient distribution at x = 20D with varying temperature. The temperature and temperature gradient distribution are symmetric about the central axis. The temperature gradient increases with an increase of the gas inlet temperature and decreases as the position moves from pipe axis to the pipe surface.

Particle Deposition Analysis

In this study, the particle transfer may be caused by the flow drag, Brownian, thermophoretic, and gravitational forces. Nanoparticles can homogeneously move with the fluid, given a slip velocity relative to the fluid. For nanoparticles, the Brownian force and thermophoretic force are the significant slip mechanisms in the transfer process. The thermophoretic force causes a non-uniform particle distribution, while Brownian forces take the particles in the opposite direction of the particle concentration gradient, trying to make the particles more homogeneous. The Brownian force and thermophoretic force oppose and affect each other. To determine the main mechanism of the nanoparticle migration, the ratio of Brownian diffusivity to thermophoretic diffusivities given different temperature gradients (N_{BT}) has been defined. The Brownian diffusivity, D_B, is expressed by the Einstein-Stokes equation as:

$$D_B = \frac{KT}{3\pi\mu_f d_p} \tag{12}$$

The thermophoretic diffusion coefficient D_T is:

$$D_T = 0.26\frac{\mu_f}{\rho_f T}\frac{\alpha_f}{2\alpha_f + \alpha_p} \tag{13}$$

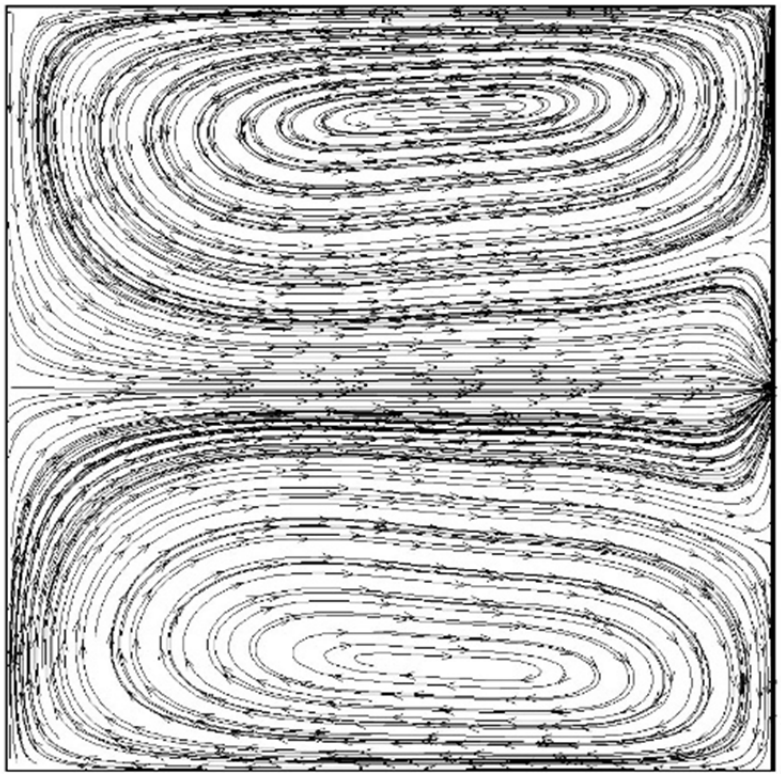

Fig. 4. Streamlines at 45° deflection cross-section with *D*e = 129.9.

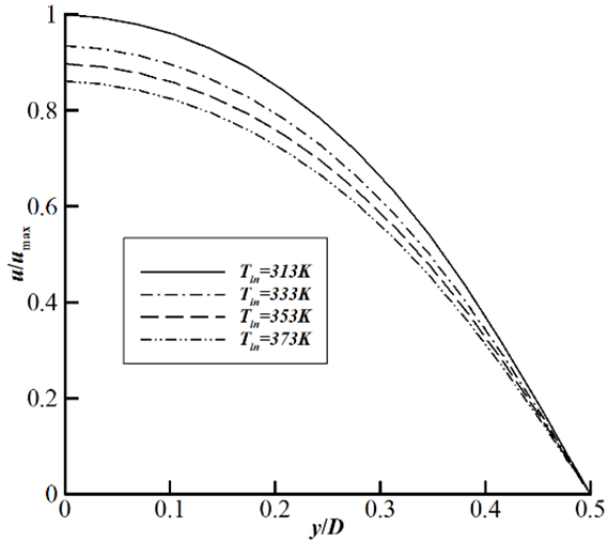

Fig. 5. The velocity distribution at x = 20 D with different gas inlet temperature.

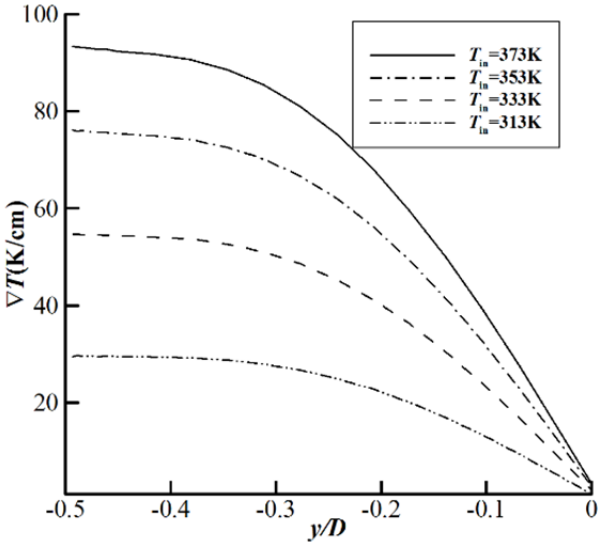

Fig. 6. The temperature gradient distribution at x = 20 D with different gas inlet temperature.

The expression of N_{BT} is (Malvandi and Ganji, 2014; Ryzhkov and Minakov, 2014):

$$N_{BT} = \frac{D_B}{D_T \nabla T} \tag{14}$$

Fig. 7 shows N_{BT} changing with particle diameter and temperature. N_{BT} decreases with particle diameter and temperature increasing. This result shows that the Brownian force plays a more important role for particle deposition with smaller particles and lower air temperatures, such as ΔT < 20°C for d_p < 100 nm, or ΔT > 60°C for d_p > 30 nm. The higher the temperature gradient, the larger the thermophoretic force will be. When ΔT > 80°C, nanoparticle migration is determined by the thermophoretic force with d_p < 100 nm. Thermophoretic force pushes the nanoparticles in the opposite direction of the temperature gradient and causes a less uniform nanoparticle distribution. Brownian force is a random force, but with higher concentration

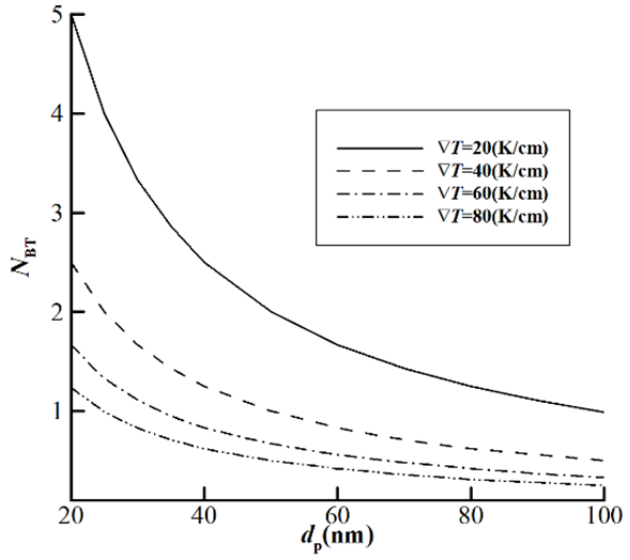

Fig. 7. The ratio of Brownian diffusivity to thermophoretic diffusivities changing with temperature and particle diameter.

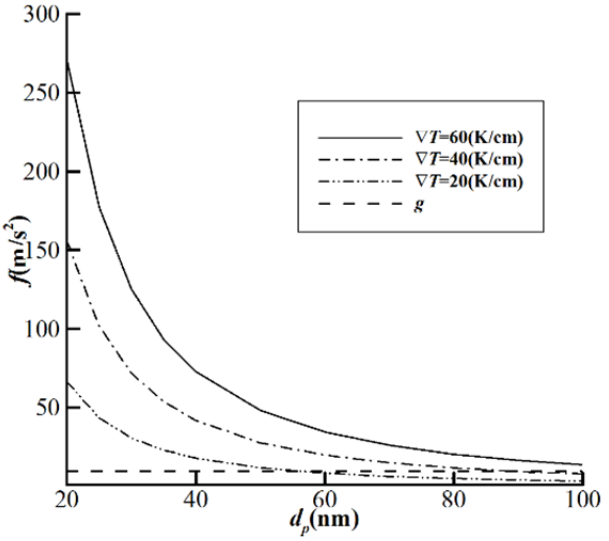

Fig. 8. The particle's acceleration changing with temperature and particle diameter.

gradients and a less uniform nanoparticle distribution, the Brownian force pushes the particles in the opposite direction of the particle concentration gradient and makes their distribution more homogeneous. In this study, the wall has been set to be lower temperature than the fluid, so that the Brownian force and the thermophoretic force oppose and affect each other near the pipe wall.

Among Brownian force, flow drag force, thermophoretic force and gravity, the thermophoretic force and gravity are always pointing towards the wall. To compare the importance of these two forces in inducing particle deposition, Fig. 8 shows a particle's acceleration because of the thermophoretic force with different temperature gradients and gravity. The result shows that with an increase of particle diameter from 20 nm to 100 nm, the particle's acceleration caused by thermophoretic force decreases rapidly. Thermophoretic acceleration is clearly affected by temperature difference, and a high temperature gradient induces high thermophoretic acceleration. When d_p < 50 nm, the value of acceleration from the thermophoretic force is greater than gravity, and the thermophoretic force dominates the particle's deposition in the presence of a temperature gradient. When d_p > 50 nm, the effect of gravity on the deposition process become more important.

In this paper, the Eulerian-Lagrangian method has been used to simulate the gas and particles flow in a steady laminar regime. Different flow conditions have been determined as functions of particle diameter and varied fluid temperatures. Once a particle hits a pipe wall it sticks to the surface. The nanoparticle deposition efficiency (n) in a bend is defined as:

$$n = N_{deposition}/N_{total} \times 100\% \quad (15)$$

where $N_{deposition}$ is the deposition particle number on the wall, and N_{total} is the number of the total particles released at the inlet. Fig. 9 shows the result of nanoparticle deposition

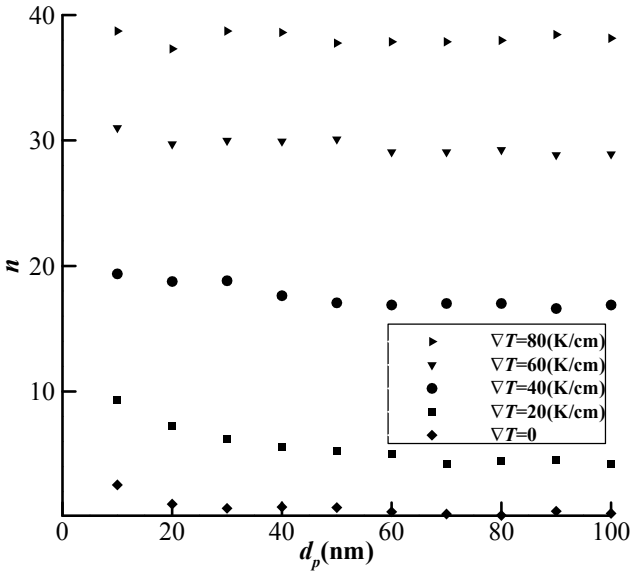

Fig. 9. The particle deposition efficiency changing with temperature and particle diameter.

efficiency changing with particle diameter and fluid inlet temperature. The figure indicates the nanoparticle deposition efficiency (n) increases with fluid temperature and only shows a small change with changing particle diameter. The nanoparticle deposition efficiency increases from < 5% with flow inlet temperature at 293 K (with a temperature gradient of 0 K) to near 40% with flow inlet temperature at 373 K and temperature gradient equal to 90 K. The former particle deposition is caused by the Brownian force and the effects of gravity. Because of the low particle concentration, the Brownian movement is random and sometimes opposite the gravity effect. As a result, the nanoparticle deposition efficiency is very low. Small particles have violent Brownian motions, giving them a high probability to hit the surface. With increasing the temperature gradient, the thermophoretic

force dominates particle deposition. As a result, the deposition efficiency increases with temperature. In Fig. 9 the Brownian movement induces the fluctuation of particle deposition efficiency with $d_p < 30$ nm.

Fig. 10 shows the nanoparticle deposition efficiency (n) changing with particle diameter at $De = 62$ and $T_{in} = 373$ K. With $d_p < 30$ nm, the result shows that Brownian movement is the main reason for particle deposition on the surface with the same temperature gradient. The particle movement is random, which leads to the nanoparticle deposition efficiency on the floor surface to be smaller than that of the ceiling surface. With increasing particle diameter, gravity becomes more significant. However, the difference of the nanoparticle deposition efficiency between the floor surface and ceiling surface becomes larger. The phenomenon of larger particles of high inertia tending to deposit on the outer wall of a curved bend is apparent in Fig. 10, because of the secondary flow structures.

CONCLUSION

This paper uses theoretical and numerical simulation methods to analyze gas-nanoparticle flows with temperature gradient which are of great importance in many technical applications. The continuous phase is predicted by applying Euler's method to the effects of temperature on fluid physical parameters. For the particulate, the discrete phase model within a Lagrangian framework is adopted to track particles through the flow field. The drag force, Brownian force, thermophoretic force and gravity have been considered to study particle deposition on the surfaces of a 90° square bend tube within the laminar region. The following conclusions were obtained:

(1) Nonaparticles deposit not only at the floor surface of the square pipe, but also at the two side walls and the ceiling. The number of the nanoparticles deposition on the bend surfaces depends on the effects of various forces.

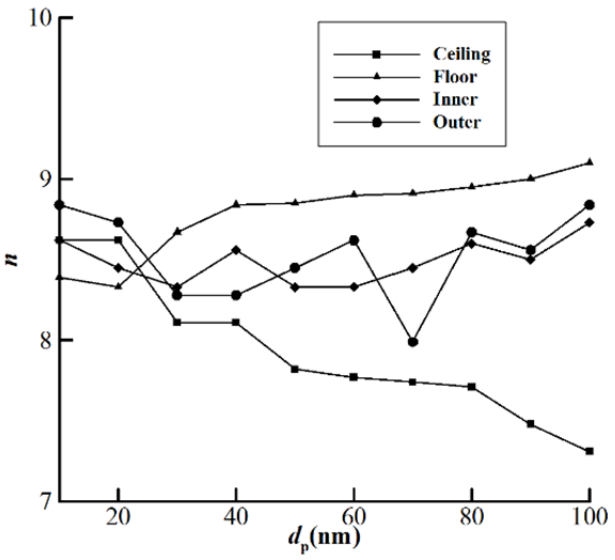

Fig. 10. The particle deposition efficiency in different surface.

(2) The Brownian force plays a more important role for particle deposition with smaller size and lower air temperature, which makes the particles more homogeneous.

(3) The thermophoretic force dominates the deposition of larger particles, which increases with temperature gradient. At the same time, gravity strongly affects particle deposition on the floor surface.

CONFLICT OF INTEREST

None declared

ACKNOWLEDGMENTS

This work is financially supported by the "National Key R&D Program of China (Grant No:2016YFF0203302)" and" National Natural Science Foundation of China (No. 11402259, No.11602266 and No.11672284)".

REFERENCES

Abarham, M., Zamankhan, P., Hoard, J.W., Styles, D., Sluder, C.S., Storey, J.M. and Assanis, D. (2013). CFD analysis of particle transport in axi-symmetric tube flows under the influence of thermophoretic force. *Int. J. Heat Mass Transfer* 61: 94–105.

Ahmadi, G. and Chen, Q. (2001). Numerical simulation of particle transport and dispersion in turbulent pipe flows. Iran. J. Sci. Technol. *Trans. B* 25: 199–219.

Breuer, M., Baytekin, H.T. and Matida, E.A. (2006). Prediction of aerosol deposition in 90° bends using LES and an efficient Lagrangian tracking method. *J. Aerosol Sci.* 37: 1407–1428.

Brock, J.R. (1962). On the theory of thermal forces acting on aerosol particles. *J. Colloid Sci.* 17: 768–780.

Buongiorno, J. (2006). Convective transport in nanofluids. *J. Heat Transfer* 128: 240–250.

Chen, W.H., Lee, K.H., Mutuku, J.K. and Hwang, C.J. (2018). Flow dynamics and $PM_{2.5}$ deposition in healthy and asthmatic airways at different inhalation statuses. *Aerosol Air Qual. Res.* 18: 866–883.

Chiou, M.C., Chiu, C.H. and Chen, H.S. (2011). Modeling particle deposition from fully developed turbulent flow. *Appl. Math. Modell.* 35: 3238–3254.

Garoosi, F., Bagheri, G. and Talebi, F. (2013). Numerical simulation of natural convection of nanofluids in a square cavity with several pairs of heaters and coolers (HACs) inside. *Int. J. Heat Mass Transfer* 67: 362–376.

Garoosi, F., Safaei, M.R., Dahari, M. and Hooman, K. (2015a). Eulerian–Lagrangian analysis of solid particle distribution in an internally heated and cooled air-filled cavity. *Appl. Math. Comput.* 250: 28–46.

Garoosi, F., Shakibaeinia, A. and Bagheri, G. (2015b). Eulerian–Lagrangian modeling of solid particle behavior in a square cavity with several pairs of heaters and coolers inside. *Powder Technol.* 280: 239–255.

Garoosi, F., Hoseininejad, F. and Rashidi, M.M. (2016). Numerical study of natural convection heat transfer in a

heat exchanger filled with nanofluids. *Energy* 109: 664–678.

Garoosi, F. and Rashidi, M.M. (2017). Two phase flow simulation of conjugate natural convection of the nanofluid in a partitioned heat exchanger containing several conducting obstacles. *Int. J. Mech. Sci.* 130: 282–306.

Garoosi, F. and Talebi, F. (2017). Numerical simulation of conjugate conduction and natural convection heat transfer of nanofluid inside a square enclosure containing a conductive partition and several disconnected conducting solid blocks using the Buongiorno's two phase model. *Powder Technol.* 317: 48–71.

Guha, A. and Samanta, S. (2014). Effect of thermophoresis and its mathematical models on the transport and deposition of aerosol particles in natural convective flow on vertical and horizontal plates. *J. Aerosol Sci.* 77: 85–101.

Gupta, G.P., Kumar, B., Singh, S. and Kulshrestha, U.C. (2016). Deposition and impact of urban atmospheric dust on two medicinal plants during different seasons in NCR Delhi. *Aerosol Air Qual. Res.* 16: 2920–2932.

Healy, D.P. and Young, J.B. (2010). An experimental and theoretical study of particle deposition due to thermophoresis and turbulence in an annular flow. *Int. J. Multiphase Flow* 36: 870–881.

Incropera, F.P. and DeWitt, D.P. (2002). *Introduction to heat transfer*, Wiley, New York.

Ketzel, M. and Berkowicz, R. (2004). Modelling the fate of ultrafine particles from exhaust pipe to rural background: An analysis of time scales for dilution, coagulation and deposition. *Atmos. Environ.* 38: 2639–2652.

Kim, M.M. and Zydney, A.L. (2004). Effect of electrostatic, hydrodynamic, and Brownian forces on particle trajectories and sieving in normal flow filtration. *J. Colloid Interface Sci.* 269: 425–431.

Li, T., Kheifets, S., Medellin, D. and Raizen, M.G. (2010). Measurement of the instantaneous velocity of a Brownian particle. *Science* 328: 1673–1675.

Lin, J.Z., Lin, P.F. and Chen, H.J. (2009a). Research on the transport and deposition of nanoparticles in a rotating curved pipe. *Phys. Fluids* 21: 122001.

Lin, J.Z., Lin, P.F., Yu M.Z. and Chen, H.J. (2010). Nanoparticle transport and coagulation in bends of circular cross section via a new moment method. *Chin. J. Chem. Eng.* 18: 1–9.

Lin, J.Z., Yin, Z.Q., Gan, F.J. and Yu, M.Z. (2014). Penetration efficiency and distribution of aerosol particles in turbulent pipe flow undergoing coagulation and breakage. *Int. J. Multiphase Flow* 61: 28–36.

Lin, P.F. and Lin, J.Z. (2009b). Prediction of nanoparticle transport and deposition in bends. *Appl. Math. Mech.* 30: 957–968.

Mädler, L. and Friedlander, S.K. (2007). Transport of nanoparticles in gases: Overview and recent advances. *Aerosol Air Qual. Res.* 7: 304–342.

Malvandi, A. and Ganji, D.D. (2014). Brownian motion and thermophoresis effects on slip flow of alumina/water nanofluid inside a circular microchannel in the presence of a magnetic field. *Int. J. Therm. Sci.* 84: 196–206.

Murgia, X., Pawelzyk, P., Schaefer, U.F., Wagner, C., Willenbacher, N. and Lehr, C.M. (2016). Size-limited penetration of nanoparticles into porcine respiratory mucus after aerosol deposition. *Biomacromolecules*. 17: 1536–1542.

Rahman, A.M., Alam, M.S. and Chowdhury, M.K. (2012). Thermophoresis particle deposition on unsteady two-dimensional forced convective heat and mass transfer flow along a wedge with variable viscosity and variable Prandtl number. *Int. Commun. Heat Mass* 39: 541–550.

Ryzhkov, I.I. and Minakov, A.V. (2014). The effect of nanoparticle diffusion and thermophoresis on convective heat transfer of nanofluid in a circular tube. *Int. J. Heat Mass Transfer* 77: 956–969.

Saidi, M. S., Rismanian, M., Monjezi, M., Zendehbad, M. and Fatehiboroujeni, S. (2014). Comparison between Lagrangian and Eulerian approaches in predicting motion of micron-sized particles in laminar flows. *Atmos. Environ.* 89: 199–206.

Schubert, M., Kita, J., Münch, C. and Moos, R. (2017). Analysis of the characteristics of thick-film NTC thermistor devices manufactured by screen-printing and firing technique and by room temperature aerosol deposition method (ADM). *Funct. Mater. Lett.* 10: 1750073.

Shams, M., Ahmadi, G. and Rahimzadeh, H. (2000). A sublayer model for deposition of nano-and micro-particles in turbulent flows. *Chem. Eng. Sci.* 55: 6097–6107.

Shimada, M., Okuyama, K. and Asai, M. (1993). Depostition of submicron aerosol particles in turbulent and transitional flow. *AIChE J.* 39: 17–26.

Shimada, M., Seto, T. and Okuyama, K. (1994). Wall deposition of ultrafine aerosol particles by thermophoresis in nonisothermal laminar pipe flow of different carrier gas. *Jpn. J. Appl. Phys.* 33: 1174.

Sommerfeld, M. (2001). Validation of a stochastic Lagrangian modelling approach for inter-particle collisions in homogeneous isotropic turbulence. *Int. J. Multiphase Flow* 27: 1829–1858.

Stapleton, K.W., Guentsch, E., Hoskinson, M.K. and Finlay, W.H. (2000). On the suitability of k–ε turbulence modeling for aerosol deposition in the mouth and throat: A comparison with experiment. *J. Aerosol Sci.* 31: 739–749.

Talbot, L., Cheng, R.K., Schefer, R.W. and Willis, D.R. (1980). Thermophoresis of particles in a heated boundary layer. *J. Fluid Mech.* 101: 737–758.

Tiwari, M., Sahu, S.K. and Pandit, G.G. (2017). PAHs in size fractionate mainstream cigarette smoke, predictive deposition and associated inhalation risk. *Aerosol Air Qual. Res.* 17: 176–186.

Tsai, C.J., Lin, J.S., Aggarwal, S.G. and Chen, D.R. (2004). Thermophoretic deposition of particles in laminar and turbulent tube flows. *Aerosol Sci. Technol.* 38: 131–139.

Vegendla, S.P., Heynderickx, G.J. and Marin, G.B. (2011). Comparison of Eulerian–Lagrangian and Eulerian–Eulerian method for dilute gas–solid flow with side inlet. *Comput. Chem. Eng.* 35: 1192–1199.

Yook, S.J. and Pui, D.Y. (2006). Experimental study of

nanoparticle penetration efficiency through coils of circular cross-sections. *Aerosol Sci. Technol.* 40: 456–462.

Zahmatkesh, I. (2008). On the importance of thermophoresis and Brownian diffusion for the deposition of micro-and nanoparticles. *Int. Commun. Heat Mass Transfer* 35: 369–375.

Zhang, Z. and Friedlander, S.K. (2000). A comparative study of chemical databases for fine particle Chinese aerosols. *Environ. Sci. Technol.* 34: 4687–4694.

Zhu, J., Tang, H., Xing, J., Lee, W.J., Yan, P. and Cui, K. (2017). Atmospheric deposition of polychlorinated dibenzo-*p*-dioxins and dibenzofurans in two cities of Southern China. *Aerosol Air Qual. Res.* 17: 1798–1810.

Received for review, February 6, 2018
Revised, April 26, 2018
Accepted, May 16, 2018